50-Gb/s ring-resonator-based silicon modulator

Takeshi Baba,[1,3,*] Suguru Akiyama,[1,3] Masahiko Imai,[1,3] Naoki Hirayama,[2,3] Hiroyuki Takahashi,[1,3] Yoshiji Noguchi,[2,3] Tsuyoshi Horikawa,[2,3] and Tatsuya Usuki[1,3]

[1]*Photonics Electronics Technology Research Association (PETRA), Japan*
[2]*National Institute of Advanced Industrial Science and Technology (AIST), Japan*
[3]*Institute for Photonics-Electronics Convergence System Technology (PECST), Tsukuba West 7, 16-1 Onogawa, Tsukuba, Ibaraki 305-8569, Japan*
[*]*t-baba@petra-jp.org*

Abstract: We achieved 50-Gb/s operation of a ring-resonator-based silicon modulator for the first time. The pin-diode phase shifter, which consists of a side-wall-grating waveguide, was loaded into the ring resonator. The forward-biased operation mode was applied, which exhibited a $V_{\pi}L$ as small as 0.28 V·cm at 25 GHz. The driving voltage and optical insertion loss at 50-Gb/s were 1.96 V_{pp} and 5.2 dB, respectively.

OCIS codes: (200.4650) Optical interconnects; (250.4110) Modulators; (250.5300) Photonic integrated circuits; (250.7360) Waveguide modulators.

References and links

1. A. F. Benner, M. Ignatowski, J. A. Kash, D. M. Kuchta, and M. B. Ritter, "Exploitation of optical interconnects in future server architectures," IBM J. Res. Develop. **49**(4), 755–775 (2005).
2. L. C. Kimerling, D. Ahn, A. B. Apsel, M. Beals, D. Carothers, Y.-K. Chen, T. Conway, D. M. Gill, M. Grove, C.-Y. Hong, M. Lipson, J. Liu, J. Michel, D. Pan, S. S. Patel, A. T. Pomerene, M. Rasras, D. K. Sparacin, K.-Y. Tu, A. E. White, and C. W. Wong, "Electronic-photonic integrated circuits on the CMOS platform," Proc. SPIE **6125**(612502), 612502, 612502-10 (2006).
3. D. A. B. Miller, "Device requirements for optical interconnects to silicon chips," Proc. IEEE **97**(7), 1166–1185 (2009).
4. Y. Urino, T. Shimizu, M. Okano, N. Hatori, M. Ishizaka, T. Yamamoto, T. Baba, T. Akagawa, S. Akiyama, T. Usuki, D. Okamoto, M. Miura, M. Noguchi, J. Fujikata, D. Shimura, H. Okayama, T. Tsuchizawa, T. Watanabe, K. Yamada, S. Itabashi, E. Saito, T. Nakamura, and Y. Arakawa, "First demonstration of high density optical interconnects integrated with lasers, optical modulators and photodetectors on a single silicon substrate," in 37th European Conference and Exposition on Optical Communications, OSA Technical Digest (CD) (Optical Society of America, 2011), paper We.9.LeSaleve.4.
5. G. T. Reed, G. Mashanovich, F. Y. Gardes, and D. J. Thomson, "Silicon optical modulators," Nat. Photonics **4**(8), 518–526 (2010).
6. S. J. Spector, C. M. Sorace, M. W. Geis, M. E. Grein, J. U. Yoon, T. M. Lyszczarz, E. P. Ippen, and F. X. Kärtner, "Operation and optimization of silicon-diode-based optical modulators," IEEE J. Sel. Top. Quantum Electron. **16**(1), 165–172 (2010).
7. M. R. Watts, W. A. Zortman, D. C. Trotter, R. W. Young, and A. L. Lentine, "Low-voltage, compact, depletion-mode, silicon Mach Zehnder modulator," IEEE J. Sel. Top. Quantum Electron. **16**(1), 159–164 (2010).
8. L. Liao, A. Liu, D. Rubin, J. Basak, Y. Chetrit, H. Nguyen, R. Cohen, N. Izhaky, and M. Paniccia, "40 Gbit/s silicon optical modulator for high speed applications," Electron. Lett. **43**(22), 1196–1197 (2007).
9. D. J. Thomson, F. Y. Gardes, Y. Hu, G. Mashanovich, M. Fournier, P. Grosse, J.-M. Fedeli, and G. T. Reed, "High contrast 40Gbit/s optical modulation in silicon," Opt. Express **19**(12), 11507–11516 (2011).
10. D. J. Thomson, F. Y. Gardes, J.-M. M. Fedeli, S. Zlatanovic, Y. Hu, B. P.-P. Kuo, E. Myslivets, N. Alic, S. Radic, G. Z. Mashanovich, and G. T. Reed, "50-Gb/s silicon optical modulator," IEEE Photon. Technol. Lett. **24**(4), 234–236 (2012).
11. W. M. Green, M. J. Rooks, L. Sekaric, and Y. A. Vlasov, "Ultra-compact, low RF power, 10 Gb/s silicon Mach-Zehnder modulator," Opt. Express **15**(25), 17106–17113 (2007).
12. S. Akiyama, T. Baba, M. Imai, T. Akagawa, M. Takahashi, N. Hirayama, H. Takahashi, Y. Noguchi, H. Okayama, T. Horikawa, and T. Usuki, "12.5-Gb/s operation with 0.29-V·cm $V\pi L$ using silicon Mach-Zehnder modulator based-on forward-biased pin diode," Opt. Express **20**(3), 2911–2923 (2012).
13. S. Akiyama, T. Baba, M. Imai, T. Akagawa, M. Noguchi, E. Saito, Y. Noguchi, N. Hirayama, T. Horikawa, and T. Usuki, "50-Gb/s silicon modulator using 250-μm-long phase shifter based-on forward-biased pin diodes," Proc. IEEE Conf. on Group IV Photonics, Paper ThC2 (2012).
14. S. Akiyama, M. Imai, T. Baba, T. Akagawa, N. Hirayama, Y. Noguchi, M. Seki, K. Koshino, M. Toyama, T. Horikawa, and T. Usuki, "Compact PIN-diode-based silicon modulator using side-wall-grating waveguide, IEEE J. Sel. Top. Quantum Electron. (submitted to).

#187131 - $15.00 USD Received 15 Mar 2013; revised 2 May 2013; accepted 2 May 2013; published 8 May 2013

15. Q. Xu, S. Manipatruni, B. Schmidt, J. Shakya, and M. Lipson, "12.5 Gbit/s carrier-injection-based silicon micro-ring silicon modulators," Opt. Express **15**(2), 430–436 (2007).
16. S. Manipatruni, Q. Xu, B. Schmidt, J. Shakya, and M. Lipson, "High speed carrier injection 18 Gb/s silicon micro-ring electro-optic modulator," in Proceedings of LEOS2007 (IEEE 2007), 537–538.
17. J.-B. You, M. Park, J.-W. Park, and G. Kim, "12.5 Gbps optical modulation of silicon racetrack resonator based on carrier-depletion in asymmetric p-n diode," Opt. Express **16**(22), 18340–18344 (2008).
18. Q. Xu, B. Schmidt, S. Pradhan, and M. Lipson, "Micrometre-scale silicon electro-optic modulator," Nature **435**(7040), 325–327 (2005).
19. F. Y. Gardes, A. Brimont, P. Sanchis, G. Rasigade, D. Marris-Morini, L. O'Faolain, F. Dong, J. M. Fedeli, P. Dumon, L. Vivien, T. F. Krauss, G. T. Reed, and J. Martí, "High-speed modulation of a compact silicon ring resonator based on a reverse-biased pn diode," Opt. Express **17**(24), 21986–21991 (2009).
20. P. Dong, S. Liao, D. Feng, H. Liang, D. Zheng, R. Shafiiha, C.-C. Kung, W. Qian, G. Li, X. Zheng, A. V. Krishnamoorthy, and M. Asghari, "Low Vpp, ultralow-energy, compact, high-speed silicon electro-optic modulator," Opt. Express **17**(25), 22484–22490 (2009).
21. S. Akiyama, T. Kurahashi, T. Baba, N. Hatori, T. Usuki, and T. Yamamoto, "A 1V peak-to-peak driven 10-Gbps slow-light silicon Mach-Zehnder modulator using cascaded ring resonators," Appl. Phys. Express **3**(7), 072202 (2010).
22. J. C. Rosenberg, W. M. Green, S. Assefa, T. Barwicz, M. Yang, S. M. Shank, and Y. A. Vlasov, "Low-power 30 Gbps silicon microring modulator," in Proceedings of Conference on Lasers and Electro-Optics / Quantum Electronics and Laser Science Conference, OSA Technical Digest (CD) (Optical Society of America, 2011), paper PDPB9.
23. G. Li, X. Zheng, J. Yao, H. Thacker, I. Shubin, Y. Luo, K. Raj, J. E. Cunningham, and A. V. Krishnamoorthy, "25Gb/s 1V-driving CMOS ring modulator with integrated thermal tuning," Opt. Express **19**(21), 20435–20443 (2011).
24. H. C. Nguyen, Y. Sakai, M. Shinkawa, N. Ishikura, and T. Baba, "10 Gb/s operation of photonic crystal silicon optical modulators," Opt. Express **19**(14), 13000–13007 (2011).
25. H. C. Nguyen, S. Hashimoto, M. Shinkawa, and T. Baba, "Sub-100 μm, 40 Gb/s photonic crystal silicon optical modulators," Proc. IEEE Conf. on Group IV Photonics, Paper PD3 (2012).
26. A. Brimont, D. J. Thomson, P. Sanchis, J. Herrera, F. Y. Gardes, J. M. Fedeli, G. T. Reed, and J. Martí, "High speed silicon electro-optical modulators enhanced via slow light propagation," Opt. Express **19**(21), 20876–20885 (2011).
27. G. Li, X. Zheng, H. Thacker, J. Yao, Y. Luo, I. Shubin, K. Raj, J. E. Cunningham, and A. V. Krishnamoorthy, "40 Gb/s thermally tunable CMOS ring resonator," Proc. IEEE Conf. on Group IV Photonics, Paper PD4 (2012).
28. X. Xiao, X. Li, H. Xu, Y. Hu, K. Xiong, Z. Li, T. Chu, J. Yu, and Y. Yu, "44-Gb/s silicon microring modulators based on zigzag pn junctions," IEEE Technol. Lett. **24**(19), 1712–1714 (2012).
29. W. D. Sacher and J. K. S. Poon, "Dynamics of microring resonator modulators," Opt. Express **16**(20), 15741–15753 (2008).

1. Introduction

High-speed and compact silicon modulators are necessary to realize large-capacity and high-density optical interconnects [1–5]. Mach-Zehnder modulators (MZMs), based on the free-carrier plasma effect, are thought to meet these demands and are most commonly investigated to achieve high-speed operation [6–14]. The injected carriers can change the refractive index of the waveguides so that the phase differences between two optical paths of the MZMs cause. There has been extensive research on achieving such high-speed MZMs by optimizing the doping profiles, as well as operating-bias voltage, of the pn- or pin-diodes. As a consequence, 50-Gb/s operation was achieved for both reverse-biased pn-diodes and forward-biased pin-diodes [10,13,14]. For both approaches described above, however, the length of the phase shifter was long and the driving voltage was high, which cannot be applied to interconnect applications.

To overcome this problem, the use of optical resonators, such as micro-ring resonators and photonic crystals, are believed promising due to the enhancement of modulation efficiency. In particular, high-speed operations up to 44 Gb/s have been reported using ring resonators [15–28]. For higher-speed operations, however, the modulation efficiency may be limited by the photon life time of the resonator [29]. To avoid this life time limitation, the Q-value of the ring resonator should not be too large or the wavelength of input light should be far from the center wavelength of the resonance. In these cases, the enhancement in modulation due to the resonator is relatively small. Thus, it is necessary to increase the modulation efficiency of the phase shifter for higher-speed operation to maintain reasonable modulation depth with low driving voltage.

#187131 - $15.00 USD Received 15 Mar 2013; revised 2 May 2013; accepted 2 May 2013; published 8 May 2013

Forward-biased pin-diodes are effective for achieving large modulation efficiency of the phase shifter in a high-frequency region [11–14]. Forward-biased diodes have sufficiently large capacitance, even for the short phase shifter in a ring resonator. Therefore, they exhibit large modulation efficiency by storing a large amount of charges for a given driving voltage. Although a pn-diode-based phase shifter shows flat frequency responses, it exhibits low-modulation efficiency of the phase shifter because of its small capacitance.

We developed a high-speed and low-driving voltage silicon modulator based on a ring resonator. The ring resonator is loaded with a phase shifter based on a side-wall grating waveguide. We used the forward-biased operation mode of pin-diodes, which exhibited a small $V_\pi L$ of 0.28 V·cm at 25 GHz. We successfully achieved 50-Gb/s operation of the fabricated modulator with a driving voltage of 1.96 V_{pp} and insertion loss of 5.2 dB. To the best of our knowledge, this is the fastest operation among ring-resonator-based modulators. In addition, 44-Gb/s operation was achieved with a driving voltage of 1.87 V_{pp} and insertion loss of 5.3 dB.

We discuss the design of our structure and the fabricating process in Section 2. In Section 3, we describe the transmission characteristics and optical frequency responses of our modulator. In Section 4, we present the experimental results of 44–50-Gb/s operation.

2. Design of silicon modulator

Figure 1 shows the top view and a scanning electron microscopy (SEM) image of our ring-resonator-based modulator. The ring consists of four straight sections and four 90-degree bends. Two pin-diode-based phase shifters, which consist of a side-wall-grating waveguide, are loaded onto the two straight sections of the ring resonator. Each phase shifter is 15-μm long. As shown in Fig. 1, narrow fins are placed at regular intervals on both sides of the waveguide core in the phase shifters. As for the design of the grating, the fins should be as narrow and long as possible for small optical loss. However, we also need low resistivity of the fins, so that the fins should be as wide and short as possible. Therefore, we chose 80-nm-wide and 1-μm-long fins, due to its constraint. The width of the waveguide core and the height of the waveguide were 450 nm and 220 nm respectively. We designed the pitch of the grating to be 284 nm, so that the operating wavelength of 1550 nm would become sufficiently larger than the Bragg wavelength of the gratings. With this condition, light propagates without serious reflection by the gratings and has almost uniform field distribution along propagation axis. Thus, the transmission spectrum of the waveguide is expected to be as flat as simple waveguide without gratings [12–14]. The radius of the corner inside the resonator is set to be 5 μm. In addition, the coupling length and the gap between resonator and the bus waveguide are 3 μm and 200 nm, respectively. With these parameters, the transmission power ratio at the coupling region was 0.87, which means 13% of input power of light is transferred from the input waveguide to the counterpart in the coupling region, so that the critical coupling condition can be obtained. In the experiments, we changed the coupling-length condition varying from 2 μm to 6 μm, and we used device which satisfied critical-coupling condition.

In the operation of the modulator, the resonance wavelength can be modulated by applying the voltage into both phase shifters. In accordance with the applied voltage, charges, such as electrons and holes, are injected into or extracted from the waveguide core in the phase shifters through the doped fins of the side-wall grating waveguides. Phosphorus (P +) and boron (B +) were implanted to form n + and n- and p + and p- regions, respectively. In addition, there are lightly p- or n-doped regions between the highly doped regions and the edge of the waveguide core, whose concentrations are 1×10^{19} and 3×10^{18} cm^{-3} to achieve high-speed operation of the phase shifters. A 1-μm-thick layer of silicon dioxide is deposited to cover the waveguide as a cladding layer. Contact windows are opened on the silicon pads, and 1-μm-thick aluminum layer is deposited to make contacts. This modulator was designed to meet the critical-coupling condition of the resonator so that a sharp and deep response of the transmission spectrum can be obtained.

#187131 - $15.00 USD Received 15 Mar 2013; revised 2 May 2013; accepted 2 May 2013; published 8 May 2013

In the fabrication process, dopants were first implanted on a flat silicon-on-insulator (SOI) substrate before waveguide fabrication. After the four implantations, dopants were activated by rapid-thermal annealing (RTA) of 10 s at 1000 °C. The procedure of ion implantation was almost the same as in our previous work [13], in which the condition was optimized for high-speed operation of up to 50 Gb/s. As shown in Fig. 1, though the distance between the highly doped region and the edge of the waveguide core was about 450 nm, there was a misalignment in the mask process, resulting in the doping regions having asymmetric profiles. After forming the doped regions, the waveguides were fabricated by combining the electron-beam lithography and dry-etching techniques. It was confirmed that the uniform periodicity of the side-wall gratings was formed, as shown in Fig. 1(c). The waveguides consists of channel waveguides. Therefore, the dry etching process was easier than with a rib waveguide because it is not necessary to control the height of the slab layer. Our modulator was fabricated in the Super-Clean-Room at AIST Tsukuba west by using technology for fabricating CMOS devices.

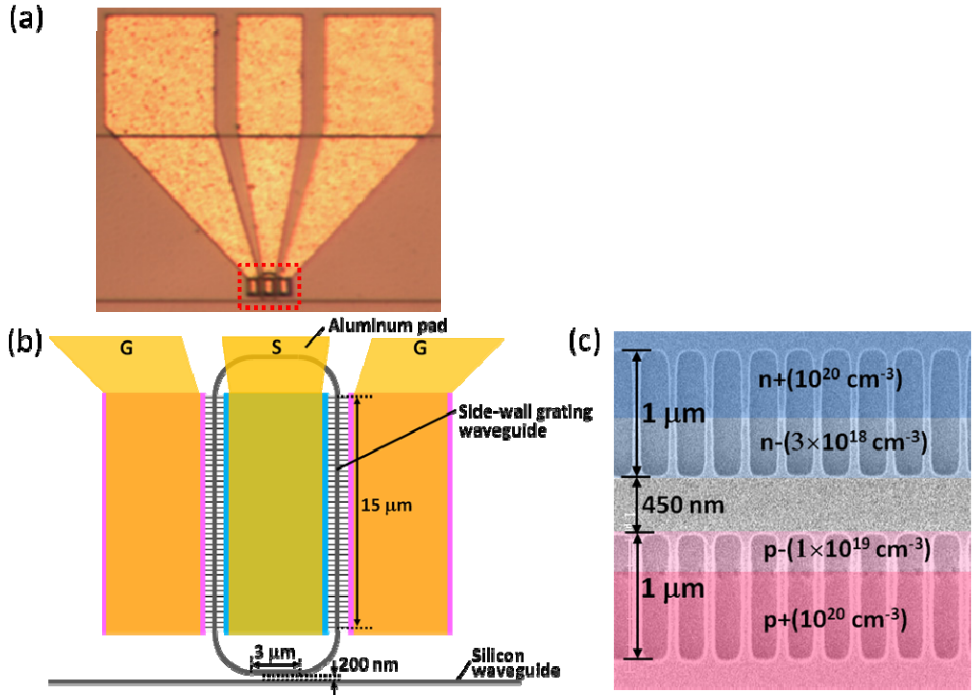

Fig. 1. (a) Top view and (b) schematic of our silicon modulator, which corresponds to dotted box in (a). (c) SEM image of fabricated phase shifter based on side-wall-grating waveguide before being covered with oxide cladding layers.

3. Measured characteristics

To characterize the resonant property of our modulator, we first measured the transmission spectrum with DC forward-bias voltages from 0 to 1.2 V. Figure 2 shows the measured spectrum. The output was normalized by the transmission intensity of the fiber-to-fiber setup, which was used for the optical couplings to the modulator. The spectrum exhibited a sharp and deep response of the resonator around 1548 nm, which indicates that critical coupling was achieved in the ring resonator. From the transmission intensity, except for the resonance wavelength, the on-chip insertion loss was about 7 dB, which includes the coupling loss between the two fibers and the waveguide. In addition, the free-spectral-range (FSR) of the resonator was 8.46 nm, as shown in the inset of Fig. 2. The resonance wavelength of the resonator shifted towards the shorter wavelength with increasing forward-bias voltage. From

#187131 - $15.00 USD Received 15 Mar 2013; revised 2 May 2013; accepted 2 May 2013; published 8 May 2013

the results of the bias voltage of 0 V, the full-width-half-maximum (FWHM) was 0.36 nm and the Q-value was 4300, which was smaller than the relatively-slow-speed modulators [15–18]. The effect of reflection at the interface between waveguides with and without the side-wall gratings was small enough that the resonant dip did not show double splitting in the spectrum. Note that the stop-band due to the side-wall grating was expected to be around 1460 nm. From the results in Fig. 2, we extracted modulation efficiency ($V_\pi L$) of the fabricated modulator at the bias-voltage of 0.92 V. We chose this bias voltage because we obtained large modulation efficiency, or large capacitance of the diodes, without causing large optical loss due to injected carriers. As shown in Fig. 2, the dip efficiently shifts for a constant change of voltage at bias voltage more than 0.9 V. However, for bias voltages more than 0.9 V, the dip became shallower due to the large optical loss caused by the injected carriers. We calculated $V_\pi L$ as follows. From the results in Fig. 2, the sensitivity of the spectral shift of the resonance to the applied bias voltage was extracted to be $\delta\lambda/\delta V$ = 1.15 nm/V around the bias-voltages of 0.92 V. This was converted to phase shift sensitivity of light by using the formula: $\delta\phi = 2\pi\delta\lambda/\mathrm{FSR}$. Therefore, the modulation efficiency ($V_\pi L$) at the DC forward bias was calculated as $V_\pi L = L\cdot\pi/(\delta\phi/\delta V) = 0.5\cdot L\cdot \mathrm{FSR}/(\delta\lambda/\delta V)$ = 0.011 V·cm, where L means the total length of the phase shifter (30 μm).

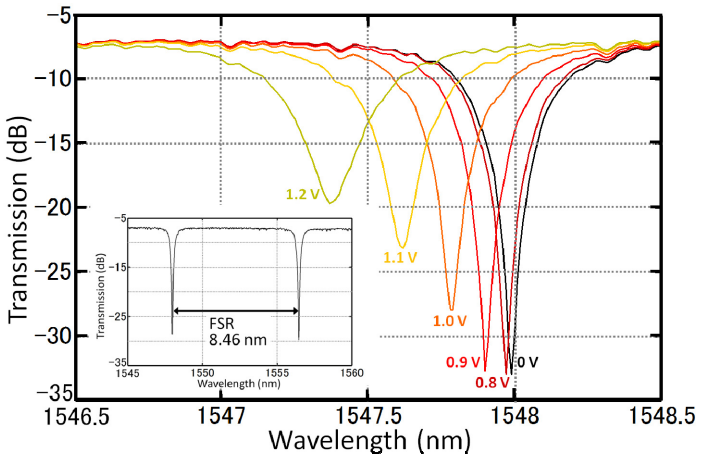

Fig. 2. Transmission spectra for various forward-bias voltages from 0 to 1.2 V. Inset shows FSR of resonator with value of 8.46 nm.

Next, we investigated the optical frequency response of the modulator for various wavelengths of the input light. Figure 3(a) shows the wavelength dependence of the optical frequency response when a forward-bias voltage of 0.92 V was applied for large capacitance and the low optical loss of the phase shifter. The wavelengths of the input light are indicated in the corresponding spectrum in Fig. 3(b). The response was large in the low frequency region below 1 GHz and decreased rapidly above that frequency [as shown in Fig. 3(a)], which is similar to general trends in modulators based on forward-biased pin-diodes. We normalized the response shown in Fig. 3 at the lowest frequency by using the measured $V_\pi L$ (0.011 V·cm) at DC. As shown in Fig. 3(a), the optical response decreases for higher frequencies. The modulation efficiency also decreases in accordance with this response curve. Therefore, we compensated this DC-$V_\pi L$ (0.011 V·cm) for the high-frequency-$V_\pi L$ considering the decreasing of the response curve obtained in Fig. 3(a). The response at 25 GHz was 28 dB lower than that at 10 MHz. The response at 10 MHz can be considered to be the same value as that at DC. Therefore, $V_\pi L$ at 25 GHz was calculated as $0.011*10^{(28/20)}$ = 0.28 V·cm. In our procedure, this high-frequency $V_\pi L$ corresponds to the efficiency of the modulator when it was operated by 25-GHz small-signal voltage in 50Ω-system. In this

#187131 - $15.00 USD Received 15 Mar 2013; revised 2 May 2013; accepted 2 May 2013; published 8 May 2013

forward-biased case, the modulation efficiency at low frequencies was large enough that the modulator maintained a relatively high efficiency near 25 GHz. This $V_\pi L$ is small compared to other reported results of diode-based silicon modulators operated over 40 Gb/s [8,10,28] and verified the high modulation efficiency of forward-biased diodes. From these results, it is expected that the fabricated modulator provides high-speed and low-voltage operation of up to 50 Gb/s by compensating for its frequency dependence. In Fig. 3(a), the shapes of the response curves are the almost same, irrespective of the input wavelengths. This implies that the photon lifetime of the resonator does not seriously affect the response of the modulator in the measured frequency range. To further investigate the effect of the photon lifetime, the optical frequency responses at the reverse-bias voltage were investigated for various wavelengths of input light. In reversed mode, the carrier dynamics is sufficiently fast due to the small capacitance; thus, small resistance-capacitance (RC) time constant. Therefore, we can easily observe the intrinsic response of the resonator. Figure 3(c) and 3(d) show the experimental results in the same manner as Fig. 3(a) and 3(b) when the reverse-biased voltage of −3 V was applied to the diode. In Fig. 3(c), the response, indicated in light blue, decreased near the 25 GHz due to the lifetime limitation of the resonator. At a small distance away from the center wavelength of the resonance, the response (green) did not decrease near 25 GHz. Far from the center wavelength, the response (orange) slightly increased. These tendencies confirm that the experimental results can be used to evaluate the effect of lifetime limitation of the resonator. The deviation of the response was small enough up to the frequency of 25 GHz. These results suggest that 50-Gb/s operation of our modulator is immune to the lifetime limitation of the resonator.

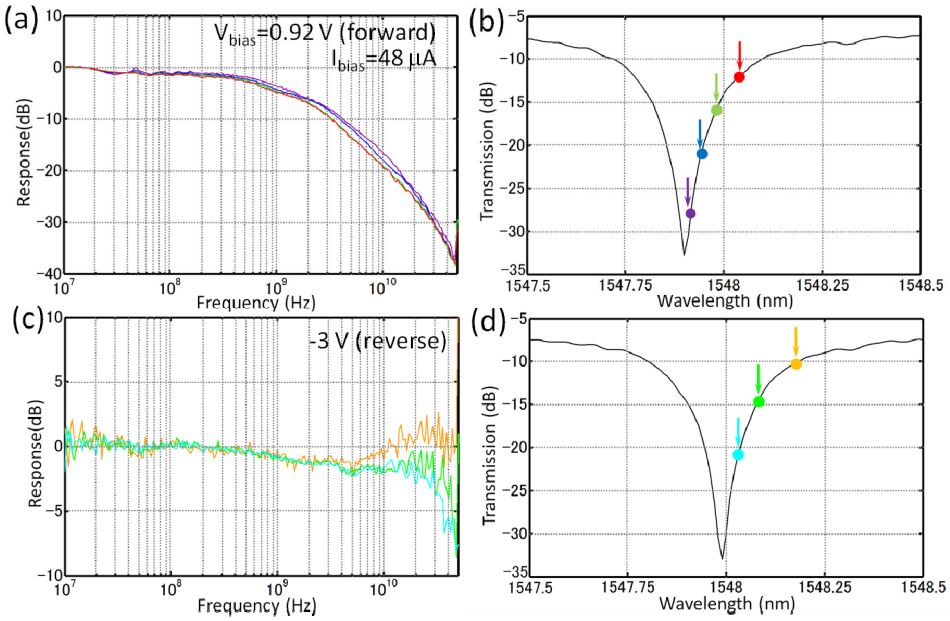

Fig. 3. , Measured optical frequency responses for various wavelengths of input light and transmission spectra of modulator. (a) Optical frequency responses and (b) transmission spectrum at forward bias condition of 0.92 V. Input wavelengths are indicated using same color plotting between (a) and (b). (c) Optical frequency responses and (d) transmission spectrum at reverse bias condition of −3 V. Input wavelengths are indicated using same manner in Fig. 3(a) and 3(b).

#187131 - $15.00 USD Received 15 Mar 2013; revised 2 May 2013; accepted 2 May 2013; published 8 May 2013

4. High-speed large-signal modulation experiment

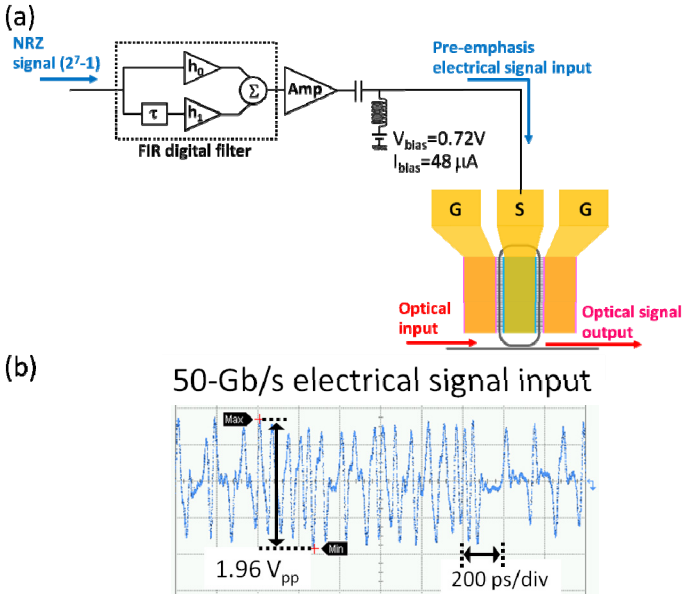

Fig. 4. (a) Setup of large-signal modulation experiment (b) 50-Gb/s pre-emphasis electrical driving signal.

We conducted a large-signal modulation experiment of the modulator by using a pseudorandom binary sequence of 2^7-1. In the experiments, the maximum operating speed was 50 Gb/s, which was upper limit of our setup. A pre-emphasis signal was used to compensate for the frequency responses of the modulator. A finite-impulse-response (FIR) digital filter was used to convert standard non-return-to-zero (NRZ) signals into pre-emphasis signals. Figure 4 shows a block diagram of the FIR-based pre-emphasis filter with two taps we used in the experiment. The FIR filter consisted of a broadband divider, constant delay (τ), multipliers (h_0 and h_1), and a combiner (Σ), as shown in Fig. 4. The transfer function $T(\omega)$ of this FIR filter is expressed as follows: $T(\omega) = h_0 + h_1\exp(-i\omega\tau)$. The parameters h_0, h_1, and τ, which we used in the 50-Gb/s operation, were 1.00, –0.91, and 10 ps [Fig. 4(a)], respectively. In Fig. 5, the calculated response curve of the FIR filter was shown.

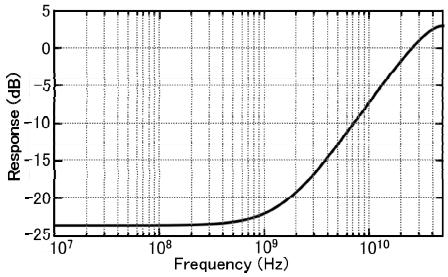

Fig. 5. Response curve of the FIR digital filter.

Figure 6(a) shows the waveform of the resultant pre-emphasis signals after being amplified. The peak-to-peak voltage (V_{pp}) was 1.96 V_{pp}, as indicated in Fig. 4(b). It was measured in a 50-Ω system, though we left the electrodes of the modulator electrically open during high-speed operation. After amplification, the signals were leveled at 0.72 V at DC to keep the diodes forward-biased in which the bias current flow (48 μA) was the same as in the

#187131 - $15.00 USD Received 15 Mar 2013; revised 2 May 2013; accepted 2 May 2013; published 8 May 2013

small-signal experiment. Figure 6(a) shows the resultant optical 50-Gb/s eye diagram. We successfully obtained eye openings at 50 Gb/s. The dynamic extinction ratio (ER) and optical insertion loss (IL) were 4.58 and 5.2 dB, respectively. In this experiment, ER means the ratio between the 0-level optical signal (P_0) and 1-level optical signal (P_1), which can be described as ER = 10 $\log_{10}(P_1/ P_0)$. To determine the IL, we measured the optical output power (I_{ref}) as a reference at the nonresonant wavelength when the diodes were kept only DC-bias without high-frequency voltage. Next, we measured the average optical-output power (I_{mod}) from the modulator during 50-Gb/s operation, whose operation wavelength was near the resonant wavelength of the ring resonator. By using these two values, IL was determined as IL = 10 $\log_{10}(I_{ref} / I_{mod})$ [indicated in the caption of Fig. 6(a)]. As far as we know, this is the first time a ring-resonator-based modulator operated at 50 Gb/s. The driving voltage, dynamic ER, and optical IL were all comparable to or even better than the other reported ring-resonator-based modulators operated at or higher than 40 Gb/s [27, 28]. As Fig. 6(b) shows, we operated the same device at 44 Gb/s using driving voltage of 1.87 V_{pp}. In this case, we chose the driving voltage to obtain about the same ERs as in case of 50 Gb/s. For 44-Gb/s case, the ER of 4.8 dB and IL of 5.3 dB were obtained. Comparing these two operating speeds, the swing voltage at 44-Gb/s was slightly smaller than that at 50-Gb/s. This is because forward-biased modulator provides larger efficiency for lower speed, as can be understood in Fig. 3(a). These results in Fig. 6 indicate that our approach to use forward-biased diodes and ring-resonator is effective to obtain high-speed and low-driving voltage modulators.

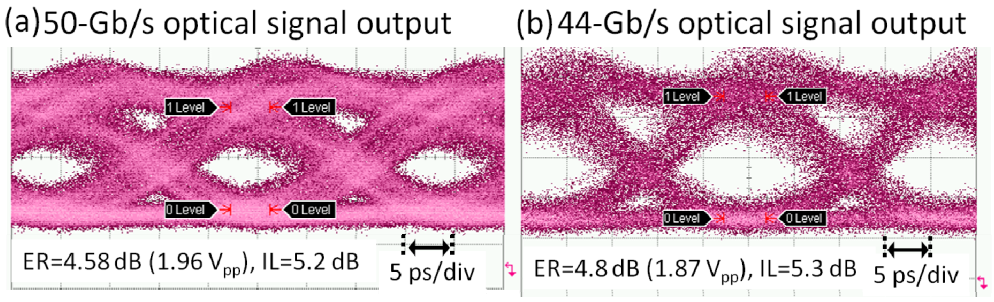

Fig. 6. (a) 50-Gb/s optical eye diagram with driving voltage of 1.96 V_{pp}. The dynamic extinction ratio (ER) was 4.58 dB. Insertion loss (IL) was 5.2 dB (b) 44-Gb/s optical eye diagram with driving voltage of 1.87 V_{pp}. ER and IL were 4.8 dB and 5.3 dB respectively. ER means the ratio between the 0-level optical signal (P_0) and 1-level optical signal (P_1), which can be described as ER = 10 $\log_{10}(P_1/ P_0)$. We used levels indicated in the graphs as "0 Level" and "1 Level" for P_0 and P_1, respectively. To determine the IL, we measured the optical output power (I_{ref}) as a reference at the nonresonant wavelength when the diodes were kept only DC-bias without high-frequency voltage. Next, we measured the average optical-output power (I_{mod}) from the modulator during 50-Gb/s operation. By using these two values, IL was determined as IL = 10 $\log_{10}(I_{mod} / I_{ref})$

5. Conclusion

We investigated the high-speed and low-voltage operation of a silicon modulator based on a ring resonator. The phase shifter consists of pin-diodes and a side-wall grating waveguide. We obtained a $V_\pi L$ as small as 0.28 V·cm at 25 GHz by using the forward-biased operation mode. We achieved 50-Gb/s operation with a dynamic ER of 4.58 dB, operated by 1.96-Vpp pre-emphasis signals and forward-bias voltage, which is, to the best of our knowledge, the fastest among reported ring-resonator-based modulators.

Acknowledgments

This research is supported by the Japan Society for the Promotion of Science (JSPS) through the "Funding Program for World-Leading Innovative R&D on Science and Technology (FIRST Program)," initiated by the Council for Science and Technology Policy (CSTP).

#187131 - $15.00 USD Received 15 Mar 2013; revised 2 May 2013; accepted 2 May 2013; published 8 May 2013